Determination of the Intrinsic Proton Binding Constants for Poly(amidoamine) Dendrimers via Potentiometric pH Titration

Yanhui Niu, Li Sun, and Richard M. Crooks*

Department of Chemistry, Texas A&M University, P.O. Box 30012, College Station, Texas 77842-3012

Received March 3, 2003; Revised Manuscript Received May 21, 2003

ABSTRACT: Protonation of fourth-generation poly(amidoamine) dendrimers terminated with hydroxyl and amine functional groups has been studied by potentiometric pH titration. The titration data are analyzed using a multishell structural model and a Frumkin adsorption isotherm to approximate proton–dendrimer binding equilibria. Site-to-site correlation is ignored, and counterions are treated according to the standard Debye–Hückel theory. This analysis yields two binding parameters: the intrinsic proton binding constant and a constant that characterizes the strength of electrostatic interactions among occupied binding sites. For the hydroxyl-terminated dendrimers, the internal tertiary amines have an average binding constant ($pK = 6.30$) 1–2 pH units lower than the value expected for a single, isolated binding site. This shift in pK is attributed to a hydrophobic microenvironment within the dendrimer interior. In contrast, no significant shift has been observed in the binding constant ($pK = 9.23$) for the peripheral primary amines in the amine-terminated dendrimer because the microenvironment around the primary amines is more hydrophilic. The strength of electrostatic interactions obtained from titration data is 3 times (primary amines) and 8 times (tertiary amines) smaller than the calculated values based on the multishell model. We hypothesize that the diminished interaction strength results from ion pairing between bound protons and counterions. In addition to the Debye–Hückel contribution from mobile ions, ion pairing provides extra Coulomb charge screening.

Introduction

Because of their unique structural topology and chemical versatility, dendrimers have found applications related to catalysis, drug delivery, energy transfer, and molecular recognition.[1–9] In many cases, these applications strongly depend on the equilibrium between dendrimers and ions, but there have only been a few experimental studies that address this issue.[10–12] Here, we present a theoretical interpretation of experimentally determined titration data for poly(amidoamine) (PAMAM) dendrimers.

We recently developed a theoretical approach, which we refer to as the "shell model", to quantify ion–dendrimer binding.[12] Some of the characteristics of this model are summarized here. First, electrostatic interactions are assumed to be the sole source of site-to-site interactions. The total energy is calculated by adopting a multishell dendrimer model, and discrete charges within each shell are summed and approximated as a shell of continuous charge. This procedure makes it possible to solve the linearized Poisson–Boltzmann (PB) equation analytically within the limit of the Debye–Hückel approximation (i.e., a dilute electrolyte solution). Second, no distinction is made between binding configurations (or microstates) that have the same set of intrashell proton binding numbers. Instead, all degenerate configurations are averaged (mean-field approximation) so that site-to-site correlations are not considered. In contrast, such a correlation is a key aspect of the Ising model that has been used previously for modeling dendrimer binding equilibria.[13] Borkovec and Koper used the Ising model to understand the protonation of poly(propyleneimine) (PPI) dendrimers, and their calculated results were found to agree fairly well with experimental NMR results.[10]

In this paper, we use the shell model to analyze experimental data from potentiometric pH titrations. Our goals are to obtain the intrinsic proton binding constants for amine groups in PAMAM dendrimers and to estimate the strength of electrostatic repulsion among occupied proton binding sites. The results indicate that interior amine groups have a smaller proton affinity compared to a single isolated amine group in the bulk electrolyte. In addition, electrostatic repulsion between occupied proton sites is weaker than that predicted by the standard electrolyte theory. Clearly, the unique microenvironment within the dendrimer interior is responsible for both of these results.

Experimental Section

Chemicals. All solutions were prepared with filtered water (18 MΩ·cm, Milli-Q, Millipore). Fourth-generation PAMAM dendrimers in methanol (Dendritech, Midland, MI), having hydroxyl or primary amine terminal groups (G4-OH and G4-NH$_2$, respectively), were dried in a vacuum to remove solvent before use. Potassium hydrogen phthalate (KHP, Fisher Scientific), Na$_2$CO$_3$, NaHCO$_3$, NaOH, concentrated HCl (EM Science), and NaClO$_4$ (Aldrich) were used as received.

Potentiometric pH Titration. A custom-built microtitrator permitted titrations to be carried out within a 1 cm cuvette of the type used for UV–vis spectroscopic measurements. The cuvette was capped with a PDMS block fitted with a pH microelectrode (U-05991-61, Cole-Parmer, Vernon Hills, IL) and tubing (0.3 mm i.d., Teflon) for titrant addition and for mixing via a gently bubbling N$_2$ stream. To minimize solution evaporation, the N$_2$ stream was presaturated with water vapor by passing it through a NaCl solution having an ionic strength similar to that of the sample solution being titrated. The temperature was maintained at 25 °C using a cuvette holder (8453A, Agilent Technologies, Palo Alto, CA) thermostated by an external water circulator (F12, Julabo, Allentown, PA). In a typical titration experiment, 600 μL of a 1.00 mM G4-OH or G4-NH$_2$ stock solution was fully protonated with excess HCl (47.6 or 95.2 μmol, respectively). Enough NaClO$_4$ (0.00, 30.0, 60.0, 150.0, or 300.0 μmol) was added to the solution to

* To whom correspondence should be addressed: voice 979-845-5629; fax 979-845-1399; e-mail crooks@tamu.edu.

increase the ionic strength by 0, 10, 20, 50, or 100 mM, respectively. The ionic strengths of acidified G4-OH and G4-NH$_2$ dendrimers prior to adding NaClO$_4$ were 15 and 29 mM, respectively.[14] The total solution volume was adjusted to 3.00 mL with water at the start of titration. NaOH titrant was added using a syringe pump (M365, Thermo Orion, Beverly, MA) at a constant rate of 0.203 μL/s, and the pH was recorded (pH 213, Hanna Instruments, Woonsocket, RI) continuously via an RS232 interface. The pH meter was calibrated daily using standard solutions (pH 4.008, 50.0 mM KHP; pH 10.012, 25.0 mM Na$_2$CO$_3$ plus 25.0 mM NaHCO$_3$).[15] NaOH (186 mM, stored under N$_2$) and HCl (238 mM) stock solutions were standardized against KHP. The precision of the titrations was consistently better than 0.5%.

Dendrimer Structural Parameters Used for Simulation. A multishell dendrimer structural model was used for the simulations.[12] Equilibrium shell diameters for G4-OH and G4-NH$_2$ dendrimers were assumed to be the same as the dendrimer diameters of the relevant generations.[16] Thus, the outermost shell of 64 terminal groups was assumed to have a diameter of 4.5 nm, identical to the diameter of a fourth-generation PAMAM dendrimer. The diameters and the number of tertiary amine groups (numbers in parentheses) for the inner shells were assumed to be 3.6 nm (32), 2.9 nm (16), 2.2 nm (8), and 1.5 nm (4). The two core nitrogen sites were combined with those in the innermost shell, and the error due to this approximation was small.[17] Other important simulation conditions are noted in the appropriate location in the text.

Results and Discussion

Brief Review of Proton–Dendrimer Binding Equilibria. We have previously shown that proton–dendrimer binding can be analyzed using a simple isotherm method, which yields simulation results equivalent to those derived from more rigorous (and complex) statistical methods.[12] In the isotherm method, only a representative or averaged binding site is considered (eq 1).

$$A + H \rightleftharpoons HA \qquad (1)$$

Here, A denotes the averaged proton binding site and H is a proton with its charge omitted for simplicity and generality. The proton binding constant β_A' for site A in the above equilibrium specifies a Frumkin adsorption isotherm (eq 2).

$$\frac{\bar{h}}{h_0 - \bar{h}} = \beta_A'[H] = 10^{pK-pH}10^{-\bar{\delta}} \qquad (2)$$

Here, $\bar{h}$ is the average proton binding number per dendrimer, h_0 is the total number of binding sites, [H] is the equilibrium concentration of proton, and pK specifies the intrinsic proton binding constant. A unitless parameter, $\bar{\delta}$, characterizes the increase in binding free energy per unit bound charge arising from site-to-site interactions, averaged over all the binding sites. Note that a list of symbols is provided at the end of the text.

Determination of Binding Parameters from Potentiometric pH Titrations. In the shell model, the proton binding number for each shell can be calculated. The sum of these binding numbers, or the average proton binding number per dendrimer, can then be compared to the experimental value. Generally, it is not possible to determine the proton binding constant for each shell because in this case the total number of adjustable parameters would exceed the number of independent parameters extractable from titration data.

Under some special conditions, however, this problem can be avoided. For example, in the case of a fourth-generation, hydroxyl-terminated PAMAM G4-OH multishell dendrimer, we can decrease the total number of adjustable parameters by assuming that all the internal tertiary amine sites have the same intrinsic proton binding constant (pK) and will experience the same free energy increase caused by site-to-site interactions ($\bar{\delta}$). With this assumption (vide infra), titration data can be linked to adjustable parameters in a very direct and transparent way. Specifically, our previous results showed that $\bar{\delta}$ varies approximately linearly with respect to the total charge Q[12] or, in this work, $\bar{h}$ (eq 3).

$$\bar{\delta} = \bar{w}Q = \bar{w}\bar{h} \qquad (3)$$

Here, $\bar{w}$ can be thought of as the average contribution of each protonated site to $\bar{\delta}$. Substituting eq 3 into eq 2 and rearranging, we obtain eq 4.

$$G(\bar{h}) = pH + \log \frac{\bar{h}}{h_0 - \bar{h}} = pK - \bar{w}\bar{h} \qquad (4)$$

A plot of $G(\bar{h})$ vs $\bar{h}$ is a straight line with an intercept of pK and a slope of $-\bar{w}$.[18,19] The function $G(\bar{h})$ is experimentally accessible because solution pH can be measured directly and $\bar{h}$ can be obtained from eq 5, which is the material balance equation for proton.

$$H_0 - B_0 - [H] + \beta_w[H]^{-1} - \bar{h}L_0 = 0 \qquad (5)$$

Here, L_0, H_0, and B_0 are the total concentrations for dendrimer ligand L (totally deprotonated state), the strong acid added initially, and the strong base (titrant) added, respectively. [H] and [OH] are linked to each other by β_w, the autodissociation constant of water. In a typical experiment, excess acid (that is, a constant H_0) is added initially, and then titration with a strong base yields a string of data pairs consisting of B_0 and [H] (or pH). Using eq 5, we can calculate $\bar{h}$ at every point along the titration curve. The validity of this approach can be tested by plotting $\bar{h}$ against $(B_0/L_0) - (H_0 - h_0L_0)/L_0$. The horizontal axis of this plot can be understood as a corrected NaOH/dendrimer molar ratio. The correction term, $(H_0 - h_0L_0)$, is the amount of strong acid in excess of the stoichiometric amount needed to titrate a completely deprotonated dendrimer. The plot should be a straight line with a slope of -1 when both [H] and [OH] are small compared to the amount of bound proton ($\bar{h}L_0$). Figure 1 shows that this is indeed the case. The intercepts of the straight line on both axes are the same (62.0) and equal to h_0 or the total number of amine groups per dendrimer molecule (also 62).

Protonation of G4-OH PAMAM Dendrimer. Proton binding to tertiary amine sites will be influenced by two factors: the inherent affinity of the site toward proton and the electrostatic repulsion between protonated sites. These two factors can be quantified by pK and $\bar{w}$, respectively (eq 4). Figure 2A shows that experimental $G(\bar{h})$ functions are linear over a wide range of $\bar{h}$, except when $\bar{h}$ approaches 0 or h_0, where the log $[\bar{h}/(h_0 - \bar{h})]$ term in eq 4 diverges quickly.[20] This linearity provides strong support for our earlier assumption that the intrinsic proton binding constants for all tertiary amine sites are roughly the same (vide supra).

pK and $\bar{w}$ are independent parameters that allow us to gain some insight into the binding chemistry and
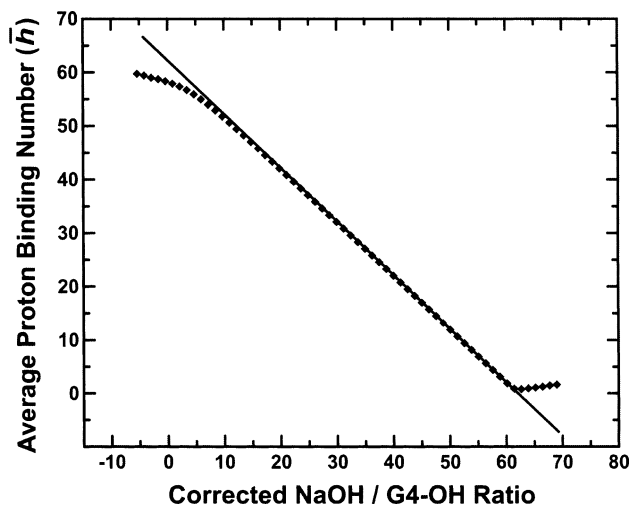
Figure 1. Average proton binding number, $\bar{h}$, as a function of the corrected NaOH/dendrimer molar ratio, or $(B_0/L_0) - (H_0 - h_0L_0)/L_0$. The points represented by diamonds are experimental data for the G4-OH dendrimer, and the solid line is the least-squares linear fit to the middle portion of the data. The intercepts on the horizontal and vertical axes are both 62.0.

structure of the G4-OH dendrimer. Equation 3 indicates that $\bar{w}$ can also be evaluated from the calculated $\bar{\delta}(\bar{h})$ (Figure 2B),[12] a function averaged over Λ charged shells as shown in eq 6.

$$\bar{\delta}(\bar{h}) = \frac{f_0 e^2}{k_B T \ln(10)} \sum_{\lambda=1}^{\Lambda} \phi_\lambda \qquad (6)$$

Here T is the absolute temperature, k_B is the Boltzmann constant, e is the charge on an electron, and f_0 is a linear scaling factor (its meaning will become apparent shortly). ϕ_λ consists of a linear combination of shell charges, q_λ, and the linear coefficients depend on many variables including the average proton binding number per dendrimer ($\bar{h}$), the ionic strength (I), the dielectric constant of the electrolyte solution (ϵ_0) and that of the dendrimer interior (ϵ), the fraction of the dendrimer volume occupied by the electrolyte solution (α), and the dendrimer dimensions (that is, the diameters of all the shells). Many of these variables are not well understood; for example, ϵ and α are difficult to estimate. Pistolis et al. have studied the dielectric properties of PAMAM dendrimer interiors using a fluorescent pyrene probe, and an estimated value of $\epsilon = 23$ can be inferred from their data.[21,22] On the basis of a report by Tomalia et al., we conclude that α is roughly 0.5 for G4 PAMAM dendrimers.[23,24]

Using the best estimates we have for various structural parameters, we can fit ($\bar{w}$) values calculated from $\bar{\delta}(\bar{h})$ to the titration data. Figure 2A shows that a good fit over ionic strengths ranging from 15 to 115 mM can be obtained, but it requires setting f_0 to 0.12. Note, f_0 is an arbitrary scaling factor included in eq 6 for the convenience of comparing experimental and theoretical $\bar{w}$ values. If our theoretical model of the dendrimer is satisfactory, then f_0 should have a value of 1. Because $\bar{w}$ specifies the strength of electrostatic interactions, a f_0 value of less than 1 can be interpreted as the observed electrostatic interactions between protonated sites being weaker than those expected from theory. However, this interpretation of f_0 depends on the assumption that the
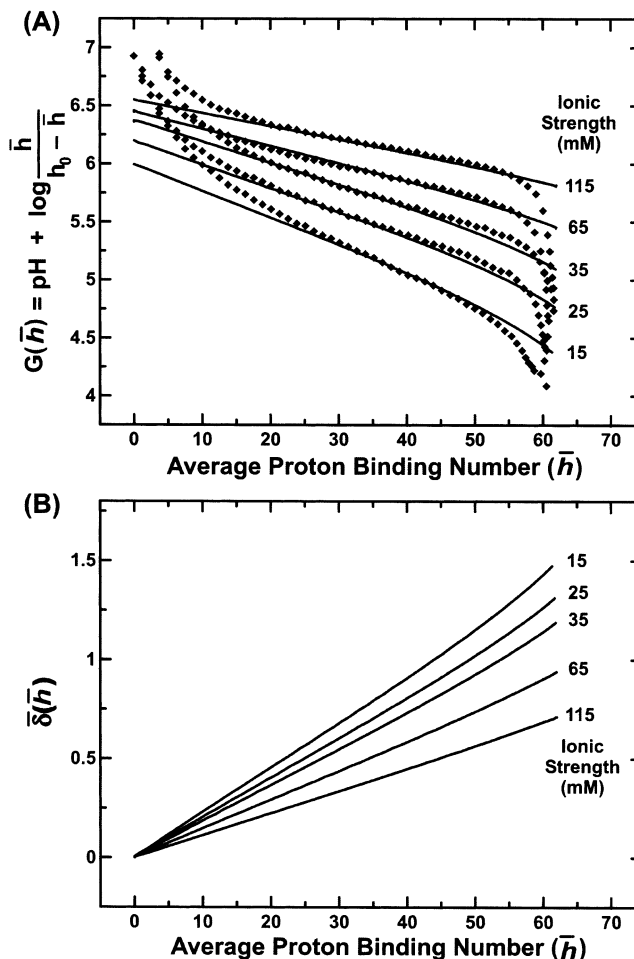
Figure 2. (A) $G(\bar{h})$ (eq 4) as a function of average proton binding number ($\bar{h}$) for the G4-OH dendrimer at the indicated ionic strengths. The data points were determined experimentally, and the solid lines are the best fits from theory. The intercepts (slopes) of these fits are 6.04 (-2.36×10^{-2}), 6.20 (-2.09×10^{-2}), 6.38 (-1.89×10^{-2}), 6.45 (-1.50×10^{-2}), and 6.55 (-1.14×10^{-2}) from ionic strength 15 to 115 mM. The scaling factor (f_0) for bound charge is 0.12 for all curves. (B) The best fits in (A) recast in terms of the function $\bar{\delta}(\bar{h})$, which is the average interaction energy per bound charge.

theoretical model itself is valid. That is, the calculated value of $\bar{w}$ should not change significantly when the adjustable parameters used for the simulation are varied over physically reasonable ranges.[21-24] In addition, we have ignored the possibility of pH-responsive changes in dendrimer size,[11,25,26] although this behavior can be easily incorporated into our algorithm. For PAMAM dendrimers, diameters will increase as pH decreases or as electrostatic repulsion increases. An expanded dendrimer would reduce the calculated value of $\bar{w}$, which would partially account for f_0 being smaller than the ideal value of 1.

Despite less than perfect knowledge of the aforementioned factors, it is still not possible to fully account for the observed large deviation in f_0 from 1. To illustrate this point, it is instructive to compare the scaling factors for a dendrimer and for a simple diamine separated by a linear alkyl spacer. As previously described,[12] the linearity of $\bar{\delta}(\bar{h})$ with respect to $\bar{h}$ is equivalent to a mean-field approximation.[13] More specifically, $\bar{w}$ used in our model is algebraically equivalent to $\epsilon^{(mf)}$ (the superscript mf stands for "mean field"), a nearest-neighbor pairwise interaction parameter used by

Borkovec and Koper.[13] For a PAMAM dendrimer, $\bar{w}$ is expected to be comparable to $\epsilon^{(mf)}$ for hexamethylene-diamine (HMDA), considering that in both cases nearest-neighbor proton binding sites are separated by six atoms or seven covalent bonds. A $\epsilon^{(mf)}$ value of 0.28 can be obtained from experimental proton binding constants ($pK_1 = 10.95$ and $pK_2 = 10.07$ at an ionic strength of 0.1 M)[27] and eq 7.[13]

$$\epsilon^{(mf)} = pK_1 - pK_2 - \log 4 \qquad (7)$$

Alternatively, an estimated $\epsilon^{(mf)}$ value of 0.19 can be derived from theory alone (eq 8).[18,28]

$$\epsilon^{(mf)} = \frac{e^2}{k_B T \ln(10)} \frac{\exp(-r_{AVG}\kappa_0)}{\epsilon_0 r_{AVG}} \qquad (8)$$

Here, r_{AVG} is the average distance between the two terminal amine sites and κ_0^{-1} is the Debye length. The agreement between the experimental and calculated $\epsilon^{(mf)}$ is remarkable because eq 8 represents a very crude approximation.[28,29] As expected, these $\epsilon^{(mf)}$ values for HMDA are comparable to $\bar{w}$ for the dendrimer (0.100 at 0.1 M ionic strength) calculated from $\bar{\delta}(\bar{h})$ using eq 6. In contrast, the experimental $\bar{w}$ (0.0114 at 0.1 M ionic strength determined using the data in Figure 2A) is about an order of magnitude smaller; that is, a f_0 value of approximately 0.1 is needed in order to fit calculated $\bar{w}$ to experimental $\bar{w}$.

The results in the previous paragraph indicate that electrostatic interactions for a simple diamine molecule can be described by the standard Debye−Hückel theory, but such a description for a multishell dendrimer overestimates the strength of electrostatic interactions between charge sites. To explore further the physical meaning of the f_0 factor, we focus our attention on eq 6. Since ϕ_λ is a linear combination of q_λ,[12] we may think of f_0 as a scaling factor for the bound charges. A small f_0, as we have seen here for G4-OH, means that the effective charges on the tertiary amine sites are smaller than expected. One possible explanation for this is that, in addition to screening by mobile ions, bound charges experience extra Coulomb screening from less-mobile counterions due to ion pairing. This hypothesis is consistent with the following information. First, the interior of a dendrimer molecule is more hydrophobic and has a smaller dielectric constant than the surrounding bulk electrolyte,[21,22] and both of these factors favor the formation of ion pairs.[30−32] Second, ion pairing only reduces the effective bound charges but does not modify the relative distribution of mobile ions. (The Debye length is independent of the magnitude of the bound charges.) It follows that, if we correct the effects of ion-pairing by choosing an appropriate f_0 factor, then the simulation results should follow the predictions of the standard Debye−Hückel theory. One such prediction is that as the ionic strength increases, the Coulomb screening by counterions will increase, resulting in a decrease in electrostatic repulsion between bound charges. Indeed, when a single scaling factor is used, calculated $\bar{w}$ values at different ionic strengths agree quantitatively with the trend predicted by theory (Figure 2A). Finally, ion pairing or "specific" ion binding has also been noticed by Huang et al., who measured the effective electrokinetic charge of a carboxylic acid-terminated dendrimer using capillary electrophoresis.[33]
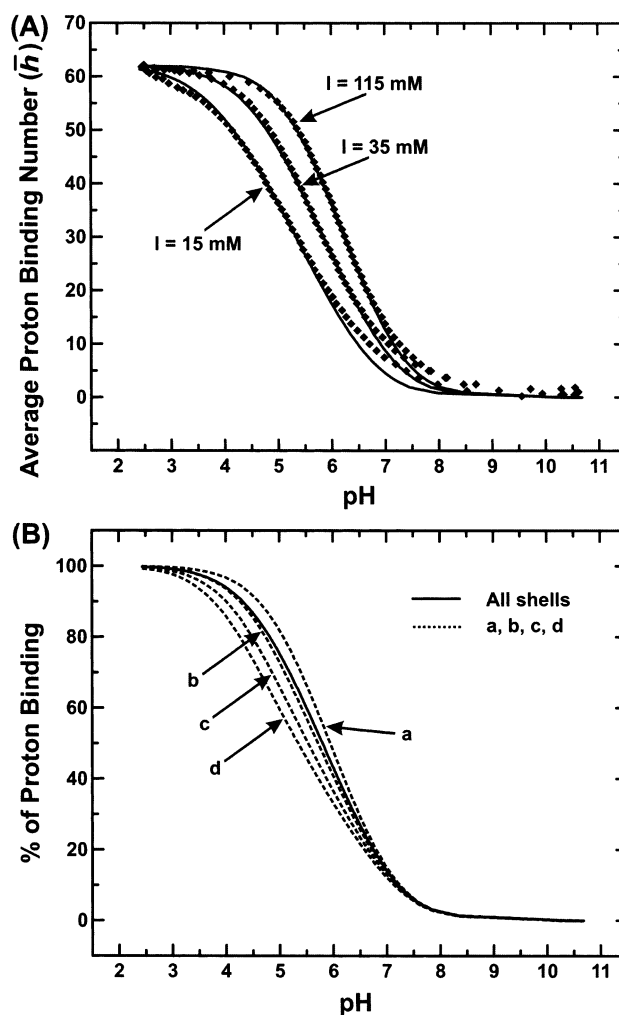
Figure 3. Alternative presentation of the data shown in Figure 2. (A) Proton binding curve for the G4-OH dendrimer, plotted as the average proton binding number vs pH, at the indicated ionic strengths. The data points are experimental data, and the solid lines are the best fits from theory. (B) Shell-level proton binding curves, plotted as the percentage of proton binding vs pH, at an ionic strength of 35 mM. The solid line represents overall binding, and the dashed lines correspond to binding at shells containing (a) 32, (b) 16, (c) 8, and (d) 6 (which includes two core sites) binding sites.

In addition to $\bar{w}$, the experimental data shown in Figure 2A also allow us to obtain the intrinsic proton binding constant of interior tertiary amines. As the ionic strength I increases, pK systematically increases from 6.00 at $I = 15$ mM to 6.65 at $I = 115$ mM. This slight increase in pK is anticipated because eq 4 has been derived with the implicit assumption that the activity coefficients for A and HA in eq 1 are neglected.[34] Compared with the pK (8.07) for a monomeric tertiary amine in a structurally similar compound,[35] the intrinsic pK for binding sites inside a dendrimer is 1−2 pH units smaller. This shift in pK is probably due to the same factors that shift the pK of a titratable residue localized within the hydrophobic pocket of some proteins.[36] That is, a hydrophobic microenvironment significantly increases the energy penalty for adding a charge to a neutral functional group.

Of particular interest to chemists is the ability to predict the degree of protonation of a dendrimer as a function of pH. Such a binding curve is essentially a plot of $\bar{h}$ vs pH (Figure 3A). Here, the experimental data agree with theoretical fits over a range of ionic strengths
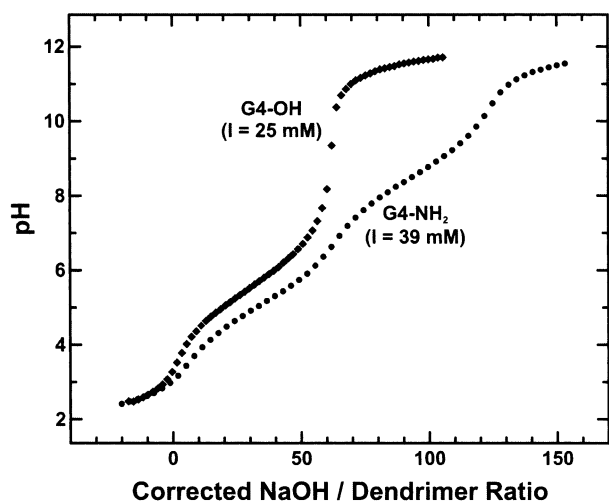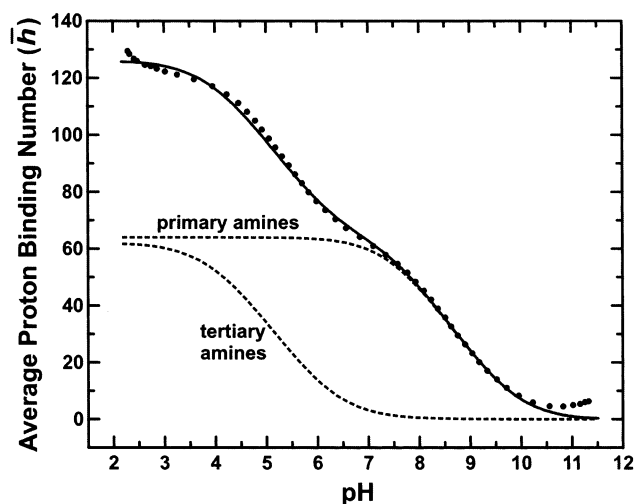
Figure 4. Potentiometric pH titration curves for G4-OH and G4-NH$_2$ at the indicated ionic strengths (I). The G4-OH curve exhibits only one end point at a molar ratio of about 62, while G4-NH$_2$ exhibits two end point transitions at molar ratios of about 62 and 126. The horizontal axis is calculated the same way as in Figure 1.

Figure 5. Proton binding curve for the G4-NH$_2$ dendrimer, plotted as the average proton binding number vs pH, at an ionic strength of 39 mM. The circles represent experimental data, the solid line is the best theoretical fit to the experimental data, and the dashed lines are shell-level binding curves for the outermost shell of 64 primary amine sites; all the inner shells contain a total of 62 tertiary amine sites. The scaling factor (f_0) is 0.35 for the primary amines and 0.12 for the tertiary amines.

from 15 to 115 mM. Generally, the slope at 50% binding increases as the ionic strength increases. When interactions between binding sites are absent, the binding curve approaches the limiting shape for an isolated single binding site. Unlike the titration data, results of calculations based on a multishell model can provide additional insight into dendrimer protonation. For example, Figure 3B shows that the pH at 50% binding for an outer shell is higher than that for an inner shell. This result is consistent with intuition because an inner-shell binding site experiences a higher degree of electrostatic interactions than an outer-shell site.[12]

Protonation of G4-NH$_2$ PAMAM Dendrimers. Results of the analysis described in the previous section for G4-OH provide a starting point for modeling protonation of the structurally related G4-NH$_2$ dendrimer. For example, we may assume that structural and binding parameters for all the tertiary amines in G4-NH$_2$ are the same as those found for G4-OH. This will leave two adjustable parameters to be determined for the peripheral primary amines: pK, the intrinsic proton binding constant, and f_0, the scaling factor for charge.[37] Again, using the titration data over a range of ionic strengths, we find that pK for the primary amines varies from 9.15 at I = 29 mM to 9.30 at I = 129 mM. These values do not differ significantly from the pK (9.28) of a monomeric analogue.[38] In addition, the best f_0 for primary amines, 0.35, is larger than that for the tertiary amines, indicating reduced specific ion pairing around the peripheral primary amines. The above results are well within intuitive expectations because a primary amine site is in close proximity with the surrounding bulk electrolyte, and thus its average microenvironment is certainly more hydrophilic than the dendrimer interior.

Because the intrinsic pKs for tertiary and primary amines differ by almost 3 pH units, we would expect the titration curve for G4-NH$_2$ to exhibit two end points corresponding to stepwise protonation of two different kinds of amine groups. The data in Figure 4 confirm this expectation. This result can be observed more clearly in binding curves ($\bar{h}$ vs pH), which include both experimental and simulation data. Figure 5 shows that

at a pH of about 7.0 most primary, but few tertiary, amines are protonated. This type of information highlights the usefulness of theoretical modeling because such information is difficult to obtain from titration data alone.

It is interesting to compare the pH-dependent proton binding properties of PAMAM and PPI dendrimers. Like G4-NH$_2$, a PPI dendrimer terminated with primary amines yields a titration curve with two end points. However, on the basis of NMR data, Koper et al. concluded that the two end points result from site-to-site correlation, which becomes significant only when electrostatic interactions between two neighboring groups are very strong.[10] Specifically, to avoid strong interactions, even-numbered dendrimer shells protonate at a different pH than odd-numbered shells, resulting in the observed two titration end points. It should be emphasized that this correlation mechanism assumes nearly identical intrinsic pK values for tertiary and primary amines; therefore, it is significantly different than the assumption underpinning the approach described in this study. If the correlation mechanism were operative for PAMAM dendrimers, then the titration curve for G4-OH would also reveal two end points. Because only one end point is actually observed, we can conclude that the correlation mechanism does not have to be considered for PAMAM dendrimers. This is understandable because the distance between two neighboring binding sites in PAMAM dendrimers is much larger than it is for PPI dendrimers; hence, weaker nearest-neighbor interactions are expected for PAMAM dendrimers. In addition, ion pairing further diminishes these nearest-neighbor interactions. Ignoring the correlation mechanism is important for us because the isotherm method used here is algebraically equivalent to adopting a mean-field approximation which, by definition, does not include site-to-site correlation. It is not possible to use titration data alone to distinguish between the two possible protonation mechanisms for PPI dendrimers because both predict a two-end-point titration curve. However, this question could be answered if PPI den-

drimers containing only internal tertiary amines were available for titration studies.

Summary

We have studied protonation of G4-OH and G4-NH$_2$ PAMAM dendrimers using both experimental and theoretical methods. Data from potentiometric pH titrations were analyzed using a multishell structural model and an isotherm binding equilibrium. Binding between protons and dendrimers is controlled by two factors: the intrinsic proton binding constant and electrostatic interactions between occupied binding sites. We found that these two factors are significantly modulated by the hydrophobic microenvironment within the dendrimer interior. Specifically, the intrinsic proton binding constant (or pK) is reduced by $1-2$ pH units, and the strength of electrostatic interactions is reduced by nearly an order of magnitude compared to a structurally similar monomeric analogue. In other words, a tertiary amine site within the dendrimer interior has a lower proton affinity than a similar site outside the dendrimer. In addition, counterions accompany the proton into the dendrimer interior, which reduces both the effective charge of bound protons and the interactions between them. Thus, an important conclusion of this study is that negatively charged counterions easily penetrate PAMAM dendrimers and reside therein.

The theoretical method used in this study is applicable to more complicated systems involving binding between metal ions and dendrimers. However, such an investigation requires a detailed understanding about dendrimer protonation, and therefore the results described here will be very useful for future studies of metal–dendrimer equilibria.[8]

Supporting Information Available: Potentiometric pH titration curves for G4-OH and G4-NH$_2$ dendrimers as a function of ionic strength. This material is available free of charge via the Internet at http://pubs.acs.org.

List of Symbols

α = fraction of the dendrimer volume occupied by the electrolyte solution

β_A' = proton binding constant for an averaged binding site

β_w = autodissociation constant of water

$\bar{\delta}$ = increase in binding free energy per unit bound charge, averaged over all the binding sites

ϵ_0 = dielectric constant of the electrolyte solution

ϵ = dielectric constant of the dendrimer interior

$\bar{h}$ = average proton binding number per dendrimer

$\epsilon^{(nf)}$ = nearest-neighbor pairwise interaction parameter used by Borkovec and Koper[13]

κ_0^{-1} = Debye length

B_0 = concentration of the strong base (titrant) added

e = charge on an electron

f_0 = arbitrary scaling factor

h_0 = total number of binding sites

H_0 = concentration of the strong acid added initially

$[H]$ = equilibrium concentration of proton

I = ionic strength

k_B = Boltzmann constant

L_0 = total concentration for dendrimer ligand L

pK = logarithm of the intrinsic proton binding constant

Q = total bound charge per dendrimer molecule

q_λ = charges on each shell

r_{AVG} = average distance between the two terminal amine sites in a simple diamine molecule

T = absolute temperature

$\bar{w}$ = slope of a plot of $\bar{\delta}$ vs $\bar{h}$

References and Notes

(1) Astruc, D.; Chardac, F. *Chem. Rev.* **2001**, *101*, 2991–3023.
(2) Kojima, C.; Kono, K.; Maruyama, K.; Takagishi, T. *Bioconjugate Chem.* **2000**, *11*, 910–917.
(3) Patri, A. K.; Majoros, I. J.; Baker, J. R., Jr. *Curr. Opin. Chem. Biol.* **2002**, *6*, 466–471.
(4) Adronov, A.; Gilat, S. L.; Fréchet, J. M. J.; Ohta, K.; Neuwahl, F. V. R.; Fleming, G. R. *J. Am. Chem. Soc.* **2000**, *122*, 1175–1185.
(5) Swallen, S. F.; Zhu, Z. G.; Moore, J. S.; Kopelman, R. *J. Phys. Chem. B* **2000**, *104*, 3988–3995.
(6) Baars, M. W. P. L.; Meijer, E. W. *Top. Curr. Chem.* **2000**, *210*, 131–182.
(7) Fréchet, J. M. J. *Proc. Natl. Acad. Sci. U.S.A.* **2002**, *99*, 4782–4787.
(8) Crooks, R. M.; Zhao, M.; Sun, L.; Chechik, V.; Yeung, L. K. *Acc. Chem. Res.* **2001**, *34*, 181–190.
(9) Gröhn, F.; Bauer, B. J.; Akpalu, Y. A.; Jackson, C. L.; Amis, E. J. *Macromolecules* **2000**, *33*, 6042–6050.
(10) Koper, G. J. M.; van Genderen, M. H. P.; Elissen-Roman, C.; Baars, M. W. P. L.; Meijer, E. W.; Borkovec, M. *J. Am. Chem. Soc.* **1997**, *119*, 6512–6521.
(11) Chen, W.; Tomalia, D. A.; Thomas, J. L. *Macromolecules* **2000**, *33*, 9169–9172.
(12) Sun, L.; Crooks, R. M. *J. Phys. Chem. B* **2002**, *106*, 5864–5872.
(13) Borkovec, M.; Koper, G. J. M. *J. Phys. Chem.* **1994**, *98*, 6038–6045.
(14) This is the ionic strength at the end of a titration, where the initial HCl is completely converted to NaCl. At the beginning of the titration, the majority of the proton from HCl binds with dendrimer, and the ionic strength is not well-defined. For example, the ionic strength is lower than the value quoted here if we exclude the contribution from the molecules being studied: i.e., charged dendrimer molecules and their associated counterions. Otherwise, a higher value will be obtained because a highly charged dendrimer molecule contributes more to ionic strength than a simple 1:1 salt.
(15) *Lange's Handbook of Chemistry*, 13th ed.; Dean, J. A., Lange, N. A., Eds.; McGraw-Hill: New York, 1985.
(16) Diameters used here are literature values measured using either size-exclusion chromatography or small-angle neutron scattering. See, for example: Crooks, R. M.; Lemon, B. I., III; Sun, L.; Yeung, L. K.; Zhao, M. *Top. Curr. Chem.* **2001**, *212*, 81–135.
(17) To quantify this error, two G3-OH models are considered. The first model consists of three proton-binding shells with the following configuration: 3.6 nm (OH-group shell), 2.9 nm (16), 2.2 nm (8), and 1.5 nm (6), where the two core N atoms are included in the innermost shell. The second model consists of four proton-binding shells with configuration: 3.6 nm (OH-group shell), 2.9 nm (16), 2.2 nm (8), 1.5 nm (4), and 0.37 nm (2), where the two N sites (ethylenediamine core) are modeled as a separate shell. Results based on the above models and other typical parameters (temperature, ionic strength, etc.) indicate that, along a typical calculated titration curve, the maximum errors in both pH and in average proton binding number are consistently less than 3%. The corresponding average errors are even smaller (<0.3%).
(18) Tanford, C. *Physical Chemistry of Macromolecules*; Wiley: New York, 1961.
(19) Equation 4 has exactly the same form as a well-known theory for analyzing protonation of colloids and polymers. In fact, $G(\bar{h})$ has already been used to model protonation of a cascade dendrimer. See, for example: Zhang, H.; Dubin, P. L.; Kaplan, J.; Moorefield, C. N.; Newkome, G. R. *J. Phys. Chem. B* **1997**, *101*, 3494–3497.
(20) The experimental $G(\bar{h})$ curve bends upward at low $\bar{h}$ values and downward at high $\bar{h}$ values. From these trends we can conclude that there exists systematic errors in experimental $\bar{h}$ values. One possible cause for these errors is that the ionic

strength of the sample solution is different than that of the standard pH solutions used to calibrate the pH meter. However, the magnitude of the error in the experimental $G(\bar{h})$ values is probably too large to be explained solely by this factor. Another possible explanation is that dendrimer dimensions are not static, as we have assumed in our model. Rather, dendrimer diameters for all the shells can expand as the degree of protonation increases. To limit the scope of this study, we have chosen to ignore pH-sensitive dendrimer expansion in this paper.

(21) Pistolis, G.; Malliaris, A.; Paleos, C. M.; Tsiourvas, D. *Langmuir* **1997**, *13*, 5870−5875.

(22) The dielectric constant was estimated using a peak ratio method. Unfortunately, the value quoted here is for a G2-NH_2 PAMAM dendrimer. An alternative probe has also been used to study the PAMAM interior up to G8 generation, but the interior dielectric constant is not quantified: Richter-Egger, D. L.; Landry, J. C.; Tesfai, A.; Tucker, S. A. *J. Phys. Chem. A* **2001**, *105*, 6826−6833.

(23) Tomalia, D. A.; Naylor, A. M.; Goddard, W. A., III *Angew. Chem., Int. Ed. Engl.* **1990**, *29*, 138−175.

(24) This is the value for a PAMAM dendrimer with an ammonia core (three branches) whereas the dendrimer we used has an ethylenediamine core (four branches). Thus, the value quoted here might be an upper limit because we expect a smaller electrolyte volume for the four-branch core.

(25) Newkome, G. R.; Young, J. K.; Baker, G. R.; Potter, R. L.; Audoly, L.; Cooper, D.; Weis, C. D.; Morris, K.; Johnson, C. S., Jr. *Macromolecules* **1993**, *26*, 2394−2396.

(26) Nisato, G.; Ivkov, R.; Amis, E. J. *Macromolecules* **2000**, *33*, 4172−4176.

(27) Martell, A. E.; Smith, R. M.; Motekaitis, R. J. *NIST Critically Selected Stability Constants of Metal Complexes*; Database 46, Version 6, 2000.

(28) This expression gives the electric potential energy around an ion according to the Debye−Hückel theory. The size of the counterions in the Debye−Hückel model is set to zero, as it is in our shell model.

(29) Only a rough estimate of r_{AVG} is used here: the average dynamic distance between two terminal amines is estimated to be 0.4 nm using established C−N and C−C bond lengths and the root-mean-square formula described in ref 18 (only applicable when the intervening C−N and C−C bonds have complete translational and rotational freedom). As expected,

this value is comparable to the average radius difference (0.35−0.45 nm) between two neighboring shells of a PAMAM dendrimer because these shells are separated by roughly the same number of covalent bonds. Other implied assumptions in eq 8 are (a) only mobile ion distribution around one of the amine sites is considered whereas (b) the other site is treated as a nonperturbing test charge.

(30) Mayer, U. *Coord. Chem. Rev.* **1976**, *21*, 159−179.

(31) Vieux, A. S.; Rutagengwa, N. *J. Phys. Chem.* **1976**, *80*, 1283−1291.

(32) Zeldovich, K. B.; Khokhlov, A. R. *Macromolecules* **1999**, *32*, 3488−3494.

(33) Huang, Q. R.; Dubin, P. L.; Moorefield, C. N.; Newkome, G. R. *J. Phys. Chem. B* **2000**, *104*, 898−904.

(34) The activity coefficient for proton H has already been included because the pH meter directly measures activity. Thus, a K determined from Figure 2A is equal to a binding constant (at infinite dilution) times γ_{HA}/γ_A, where γ_{HA} and γ_A are activity coefficients. For a neutral binding ligand A (i.e., the amine), HA would be positively charged: so γ_{HA} is expected to be smaller than γ_A, and the ratio γ_{HA}/γ_A will decrease as ionic strength increases. As a result, pK will increase as ionic strength increases.

(35) The compound, denoted as M_1 in the following reference, contains a tertiary amine connected to two amide bonds through ethylene linkers: Barbucci, R.; Casolaro, M.; Danzo, N.; Beni, M. C.; Barone, V.; Ferruti, P. *Gazz. Chim. Ital.* **1982**, *112*, 105−113.

(36) Mehler, E. L.; Fuxreiter, M.; Simon, I.; Garcia-Moreno, E. B. *Proteins* **2002**, *48*, 283−292.

(37) We have been careful to not overspecify the number of adjustable parameters. Here, only two scaling factors are chosen: one for the charges on the outmost shell and the other for charges in all the inner shells. These factors can be determined reliably from the two sets of titration data for G4-OH and for G4-NH_2. However, this might not be the case if more scaling factors (e.g., one for each shell) were used.

(38) The compound we selected is *N*-acetylethylenediamine: a primary amine linked to one amide bond through an ethylene linker. Its pK is 9.28. See: Hall, H. K., Jr. *J. Am. Chem. Soc.* **1956**, *78*, 2570−2572.